AMERICAN SOCIETY FOR MICROBIOLOGY | Journal of Virology®

VACCINES AND ANTIVIRAL AGENTS

Reduction of Kaposi's Sarcoma-Associated Herpesvirus Latency Using CRISPR-Cas9 To Edit the Latency-Associated Nuclear Antigen Gene

For Yue Tso,[a] John T. West,[a] Charles Wood[a]

[a]Nebraska Center for Virology and the School of Biological Sciences, University of Nebraska—Lincoln, Lincoln, Nebraska, USA

ABSTRACT Kaposi's sarcoma-associated herpesvirus (KSHV) is the etiologic agent of Kaposi's sarcoma (KS), an AIDS-defining cancer in HIV-1-infected individuals or immune-suppressed transplant patients. The prevalence for both KSHV and KS are highest in sub-Saharan Africa where HIV-1 infection is also epidemic. There is no effective treatment for advanced KS; therefore, the survival rate is low. Similar to other herpesviruses, KSHV's ability to establish latent infection in the host presents a major challenge to KS treatment or prevention. Strategies to reduce KSHV episomal persistence in latently infected cells might lead to approaches to prevent KS development. The CRISPR-Cas9 system is a gene editing technique that has been used to specifically manipulate the HIV-1 genome but also Epstein-Barr virus (EBV) which, similar to KSHV, belongs to the *Gammaherpesvirus* family. Among KSHV gene products, the latency-associated nuclear antigen (LANA) is absolutely required in the maintenance, replication, and segregation of KSHV episomes during mitosis, which makes LANA an ideal target for CRISPR-Cas9 editing. In this study, we designed a replication-incompetent adenovirus type 5 to deliver a LANA-specific Cas9 system (Ad-CC9-LANA) into various KSHV latent target cells. We showed that KSHV latently infected epithelial and endothelial cells transduced with Ad-CC9-LANA underwent significant reductions in the KSHV episome burden, LANA RNA and protein expression over time, but this effect is less profound in BC3 cells due to the low infection efficiency of adenovirus type 5 for B cells. The use of an adenovirus vector might confer potential *in vivo* applications of LANA-specific Cas9 against KSHV infection and KS.

IMPORTANCE The ability for Kaposi's sarcoma-associated herpesvirus (KSHV), the causative agent of Kaposi's sarcoma (KS), to establish and maintain latency has been a major challenge to clearing infection and preventing KS development. This is the first study to demonstrate the feasibility of using a KSHV LANA-targeted CRISPR-Cas9 and adenoviral delivery system to disrupt KSHV latency in infected epithelial and endothelial cell lines. Our system significantly reduced the KSHV episomal burden over time. Given the safety record of adenovirus as vaccine or delivery vectors, this approach to limit KSHV latency may also represent a viable strategy against other tumorigenic viruses and may have potential benefits in developing countries where the viral cancer burden is high.

KEYWORDS CRISPR-Cas9, Kaposi's sarcoma-associated herpesvirus, LANA, latency

Kaposi's sarcoma (KS) is a soft tissue tumor most commonly found in immunosuppressed individuals, such as immunodeficiency caused by HIV-1 or upon immune suppression in transplant patients (1). KS associating with HIV-1 infection is known as epidemic KS which is characterized by rapid progression and a wide distribution involving skin, viscera, and lymph nodes (2). Pleiotropic chemotherapy is the most common treatment of KS, but the long-term prognosis is generally poor (3). A recent

Citation Tso FY, West JT, Wood C. 2019. Reduction of Kaposi's sarcoma-associated herpesvirus latency using CRISPR-Cas9 to edit the latency-associated nuclear antigen gene. J Virol 93:e02183-18. https://doi.org/10.1128/JVI.02183-18.

Editor Richard M. Longnecker, Northwestern University

Address correspondence to Charles Wood, cwood1@unl.edu.

Received 6 December 2018
Accepted 3 January 2019
Accepted manuscript posted online 16 January 2019
Published 21 March 2019

study from South Africa had indicated a 2-year survival rate of less than 80% with chemotherapy or radiotherapy (4). The KS epidemic has run parallel to the HIV-1 epidemic, especially in sub-Saharan Africa where the HIV-1/AIDS epidemic continues and antiretroviral therapy (ART) has only recently become more widely available (5).

Kaposi's sarcoma-associated herpesvirus (KSHV) or human herpesvirus 8 (HHV-8) is the etiologic agent of KS. KSHV DNA has consistently been detected in biopsy samples from patients with all types of KS, and the virus is also associated with two other neoplastic disorders, namely, primary effusion lymphoma and multicentric Castleman's disease (6, 7). KSHV contains a large double-stranded DNA genome approximately 165 kb in size with approximately 90 open reading frames (ORFs) and can infect multiple cell types that manifest into different neoplastic manifestations (8). KS, for example, is primarily associated with KSHV infection of endothelial cells (9–11). The seroprevalence of KSHV is very high in Africa and parallels the incidence of KS. Studies from our laboratory, as well as others, indicate that KSHV seroprevalence can be as high as 70% in a number of African countries (12, 13). Given the millions of KSHV-infected individuals, there is a potential for them to develop KS upon immune suppression. Therefore, there is an urgent need for strategies to reduce or eliminate KSHV infection from these individuals before the development of KS.

Similar to other herpesviruses, the replication cycle of KSHV involves both a lytic and a latent phase. During latency, a reduced repertoire of viral genes, those involved in immune evasion and maintenance of the viral episome, are expressed. This reduced expression enables KSHV to establish life-long infection with latent reservoirs that can sporadically reactivate to lytic viral replication and release of progeny virions (14–17). Lytic replication leads to viremia and transmission and is correlated with KS development (18, 19). Among the latency-related viral genes, the latency-associated nuclear antigen (LANA) encoded by ORF73 plays a critical role in the maintenance, replication, and partitioning of the viral episome during mitosis (14, 17, 20, 21). Additionally, LANA alters several cellular signal pathways, interacts with tumor suppressors, such as p53 and pRb, and suppresses lytic replication (22–27). The seminal importance of LANA in the maintenance of the viral episome and latency in the infected host makes it an ideal target for therapeutic modulation, not only for KS patients but also for individuals latently infected with the virus.

The clustered regularly interspaced short palindromic repeat (CRISPR) coupled with Cas9 RNA-guided DNA nuclease from *Streptococcus pyogenes* is a flexible system that allows precise targeting and editing of specific DNA sequences within organisms when introduced ectopically (28). CRISPR is composed of a target-specific guide RNA (gRNA) and a CRISPR-associated endonuclease, such as Cas9, and together it is known as CRISPR-Cas9. Cas9 is an endonuclease that will only cleave a targeted locus if the gRNA recognizes and binds to a specific targeted sequence in the DNA. The DNA cleavage mediated by Cas9 is typically a double-stranded break that is subsequently repaired by host nonhomologous end joining (NHEJ) (28). The error-prone NHEJ pathway often results in the addition and/or deletion of nucleotides, leading to random mutations in the open reading frame of the targeted gene. These mutations can cause an alteration or loss of function in the resulting protein. Given the tremendous impact CRISPR-Cas9 has had on genome editing, it is not surprising that this technology has been tested against several latency-prone viruses, such as herpes simplex virus, human papillomavirus, and EBV, in attempts to mutate various viral proteins (29–33). Beyond these DNA viruses, it was recently shown that CRISPR-Cas9 targeting was able to eliminate HIV-1 from human $CD4^+$ T cells *in vitro*, demonstrating the potential of CRISPR-Cas9 systems in the specific targeting of latent viruses (34). These reports suggested the potential utility of CRISPR-Cas9 in editing the genes of KSHV, which is a member of the gammaherpesvirus subgroup along with EBV.

Several *in vitro* studies had demonstrated that short hairpin RNA (shRNA) silencing of LANA expression or the transient expression of the mutated LANA protein can negatively affect KSHV episomal maintenance (35, 36). However, these methods are not realistic for clinical applications. For example, lentiviral vector delivery of LANA-specific

shRNA poses the potential disadvantage of insertional mutation (37). Contrary to shRNA, the CRISPR-Cas9 system was shown to have high therapeutic potential by precise editing of their targeted genes *in vivo* in animal models (38–40). To take advantage of the power of the CRISPR-Cas9 system for genome editing, we designed a proof-of-concept approach to test the *in vitro* efficacy of replication-incompetent adenovirus type 5 delivery of a novel CRISPR-Cas9 system specifically targeting the KSHV LANA gene (CC9-LANA). We show here that the CC9-LANA system resulted in editing of the KSHV LANA gene and a resulting lack of functional LANA protein that appears to be preventing proper segregation of KSHV episomes during cell replication. We detected daughter cells without viral episomes and an overall decrease in the KSHV copy number per cell over time. Our findings suggest that the CC9-LANA system can indeed target and reduce KSHV latency and should, therefore, be tested further for *in vivo* efficacy.

RESULTS

Construction of a replication-incompetent adenovirus type 5 encoding the KSHV LANA-specific CRISPR-Cas9. To test the feasibility of targeting the KSHV LANA gene with CRISPR-Cas9, we designed a gRNA specifically targeting the N terminus of the LANA gene (nucleotide position 139 to 158). This region was selected since any mutation or deletion here will likely truncate or lead to frameshift of the ORF. The gRNA was then cloned into a shuttle vector under the control of the human U6 (hU6) promoter. A separate shuttle vector with expression driven by the human ubiquitin C (hUBC) promoter, followed by either the gene for the active or inactive form of Cas9 with the sequence for a T2A self-cleaving peptide at its C terminus, and then followed by the gene for green fluorescence protein (GFP). Although hUBC is a relatively weak promoter, it was chosen because of its advantages in reducing the off-target effects that are linked to Cas9 overexpression (41–43). In addition, the lower expression of Cas9 may benefit future *in vivo* applications by reducing elicitation of host responses against the Cas9 enzyme. Both the KSHV LANA-specific gRNA and active or inactive Cas9 were then cloned into the replication-incompetent human adenovirus type 5 vector, and the recombinant adenovirus encoding either the active (Ad-CC9-LANA) or inactive (Ad-iCC9-LANA) Cas9 was generated as described in the Materials and Methods (Fig. 1A).

Droplet digital PCR analysis of the effects of CC9-LANA on KSHV episome burden. To determine the efficiency with which CC9-LANA targeted the N terminus of the KSHV LANA gene, we designed multiple droplet digital PCR (ddPCR) primers and probes to detect the gRNA target site and other areas within the LANA gene or the ORF26 gene, which was not predicted to be affected by editing (Fig. 1B). Probe number 1 shares the same sequence as the targeted site. Probe numbers 2 and 3 are located within the LANA gene but were outside the targeted region of CC9-LANA, while probe number 4 is located in the KSHV ORF26 gene (Fig. 1B). These primers and probes supported the quantification of the impact of CC9-LANA on KSHV episomal copy number per cell. We envisioned three potentially distinct scenarios for the KSHV episome in the presence of the CC9-LANA editing complex (Fig. 1C). In the first, CC9-LANA has no effect, resulting in the KSHV episome remaining as wild type, unedited, and stable. In this case, all four probes will bind to their respective target sequences and be detected by ddPCR. The KSHV episomal copy number per cell derived from the four probes would be similar, reflecting the presence of equimolar targets (Fig. 1D). In the second scenario, the LANA target site is recognized and cleaved by CC9-LANA, followed by the introduction of random mutations from the host NHEJ pathway repairs (Fig. 1C). In this case, probe number 1 will not bind to its target sequence due to mismatches and, therefore, will not be detected by ddPCR. In contrast, probe numbers 2, 3, and 4 will bind their respective target sequences and be detected by ddPCR. A comparison of the KSHV episomal copy number per cell derived from probe number 1 to the signal derived from probe numbers 2, 3, and 4 will provide the frequency/efficiency of CC9-LANA-mediated editing (Fig. 1D). In a third scenario, the targeted site in LANA is recognized and cleaved by CC9-LANA but was not repaired,

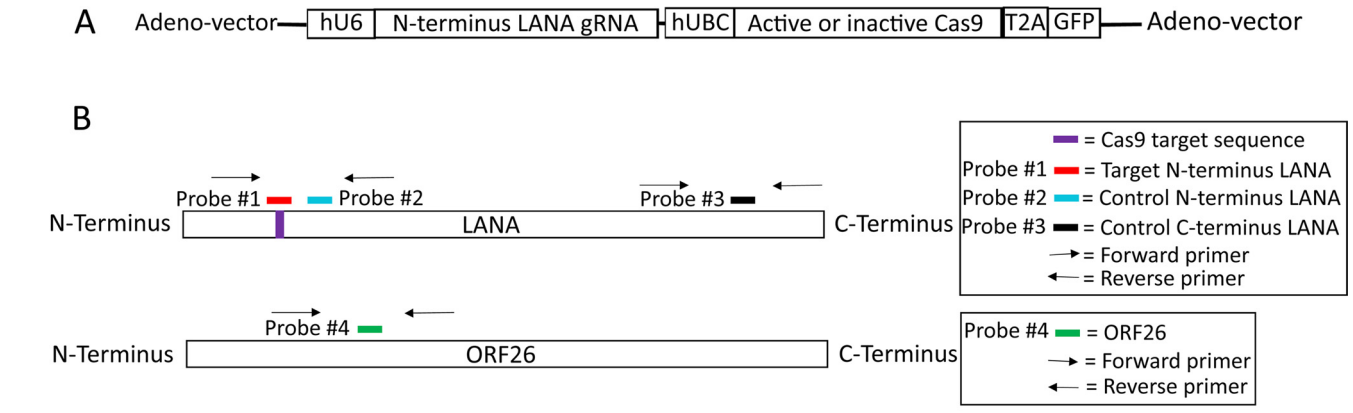

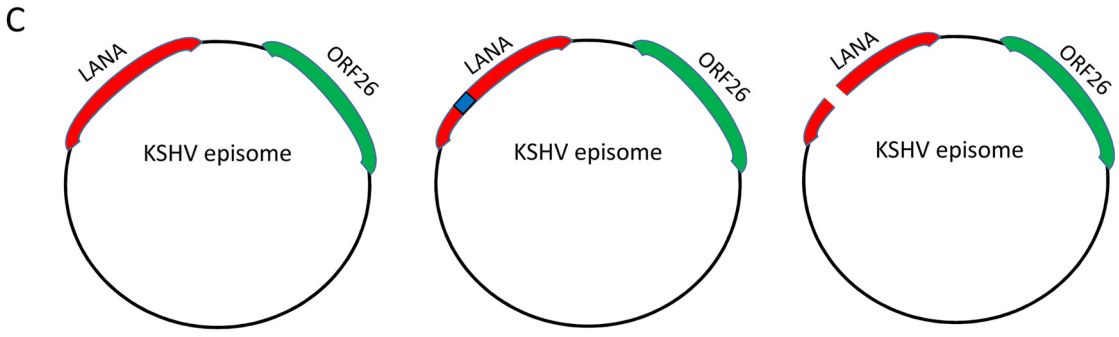

Scenario #1
Wild type

Probes	ddPCR detection
#1	Yes
#2	Yes
#3	Yes
#4	Yes

Scenario #2
Target site cleaved by Cas9
&
Repaired by host NHEJ*

Probes	ddPCR detection
#1	No
#2	Yes
#3	Yes
#4	Yes

Scenario #3
Target site cleaved by Cas9

Probes	ddPCR detection
#1	No
#2	No
#3	Yes
#4	Yes

*NHEJ = non-homologous end joining pathway

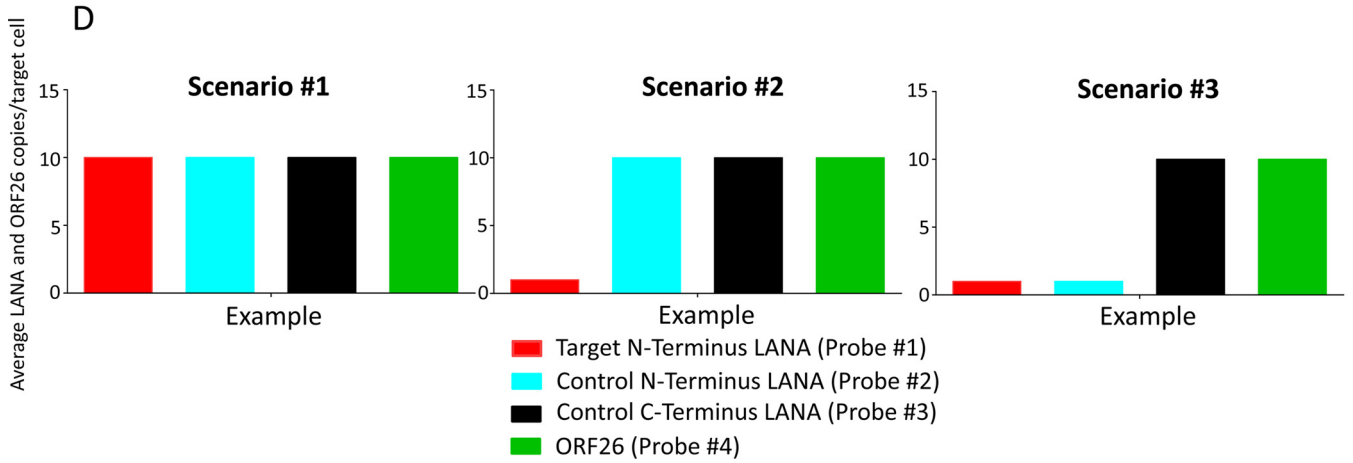

FIG 1 Illustrations of the replication-incompetent adenovirus vector and KSHV episome copy number analysis using droplet digital PCR (ddPCR). All diagrams are not drawn to scale. (A) Schematic showing the LANA-specific guide RNA and Cas9 expression cassette (CC9-LANA) in the replication-incompetent adenovirus type 5 vector. (B) Relative locations of the ddPCR amplification primers and probes within KSHV LANA and ORF26 genes. (C) The effects of a functional CC9-LANA might have on KSHV episome are presented as three hypothetical scenarios. Predicted ddPCR detectability of the respective probes are shown in tables below each scenario. (D) Example patterns of KSHV episome copy number/cell based on ddPCR analysis that reflects each hypothetical scenarios are shown.

resulting in a linearized KSHV episome that will likely be degraded over time (Fig. 1C). In this case, probe number 1 will not bind to its target sequence since it has been cleaved. Additionally, probe number 2 will also fail to be detected since its 5′ amplification primer is upstream of the cleaved site in LANA. However, probe numbers 3 and 4 will continue to bind and be detected by ddPCR. This outcome will be detected by a reduction in signal with probe numbers 1 and 2, relative to the robust detection of probe numbers 3 and 4 (Fig. 1D).

Dose-dependent CC9-LANA reduction of KSHV latent infection. As mentioned previously, KS is primarily of endothelial origin. In order to test the effectiveness of CC9-LANA in reducing the KSHV episome from latently infected cells, we needed relevant epithelial or endothelial cell lines that harbor latent KSHV. The *in vitro* models of KSHV epithelial and endothelial latent infection are limited, with the exception for Vero219, which is a kidney epithelial line from an African green monkey, *Cercopithecus aethiops*. Vero219 cells are stably infected with KSHV and maintain the KSHV episome in a latent state under puromycin selection (44). Therefore, we selected Vero219 as the first *in vitro* model for efficacy testing. To prevent puromycin from killing cells that might have lost their KSHV episomes due to CC9-LANA editing, it was removed during all transduction with the recombinant adenovirus and for subsequent culturing of these cells. We first transduced Vero219 with 10, 50, or 100 multiplicity of infection (MOI) of Ad-CC9-LANA or Ad-iCC9-LANA. Cells were collected on days 2, 6, and 11 postransduction. Genomic DNA was extracted, and the effects of active CC9-LANA on the KSHV copy number were determined in comparison with transductions with inactive CC9-LANA using ddPCR.

As expected, the overall KSHV episome burden in the cells decreased with time due to the lack of puromycin selection for the viral genome. At day 2 postransduction, the mock-transduced cells had an average of ~59 LANA and ORF26 copies/cell. This number was similar among all 4 probes and matched with scenario number 1 with no effect (Fig. 2A). However, as we had projected, both the LANA and ORF26 copy numbers decreased significantly in cells transduced with various MOI of Ad-CC9-LANA compared with that of the respective mock transduced cultures (*P* values ranged from =0.0002 to <0.0001) (Fig. 2A). At 100 MOI, the LANA and ORF26 decreased to ~48 copies/cell based on signal from probe numbers 3 and 4. This result represented a 19% reduction of KSHV episome burden in Ad-CC9-LANA versus the respective mock-transduced culture (percent reduction), as defined in Table 1. Since probe numbers 3 and 4 represent the overall KSHV episome burden, while probe number 2 represents unedited as well as edited episome, the differences between these probes will indicate the levels of episomes that were cleaved by CC9-LANA but remain linearized. At 100 MOI, probe number 2 showed ~31 LANA copies/cell that represented 35% of linearized KSHV episome (percent linearized) in the Ad-CC9-LANA-transduced culture, as defined in Table 1. More importantly, probe number 1 detected only ~15 wild-type LANA copies/cell, suggesting that 69% of the KSHV episomes in Ad-CC9-LANA-transduced culture (percent edited) at 100 MOI had been targeted and edited by CC9-LANA, as defined in Table 1. These effects were dose dependent, as demonstrated by a gradual decrease in episomal copy numbers with increasing MOI (Fig. 2A). In contrast, episomal copy number remained consistent at ~55 copies/cell in cultures transduced with various MOIs of Ad-iCC9-LANA at the same time points (Fig. 2B). These findings demonstrate that the decrease in episomal copy number observed with CC9-LANA indeed resulted from its LANA-targeted editing.

Critically, the remarkable but somewhat modest KSHV episome editing effects became more pronounced with time. At day 11 postransduction, the mock-transduced culture had slightly lower KSHV episome burden due to a lack of puromycin selection but still at an average of ~45 LANA and ORF26 copies/cell (Fig. 2A). However, in cells transduced with Ad-CC9-LANA at 100 MOI, LANA and ORF26 had been reduced to ~28 copies/cell, representing 38% reduction (Fig. 2A). Meanwhile, probe number 2 quantification indicated a further decrease in LANA to 19 copies/cell, representing 32%

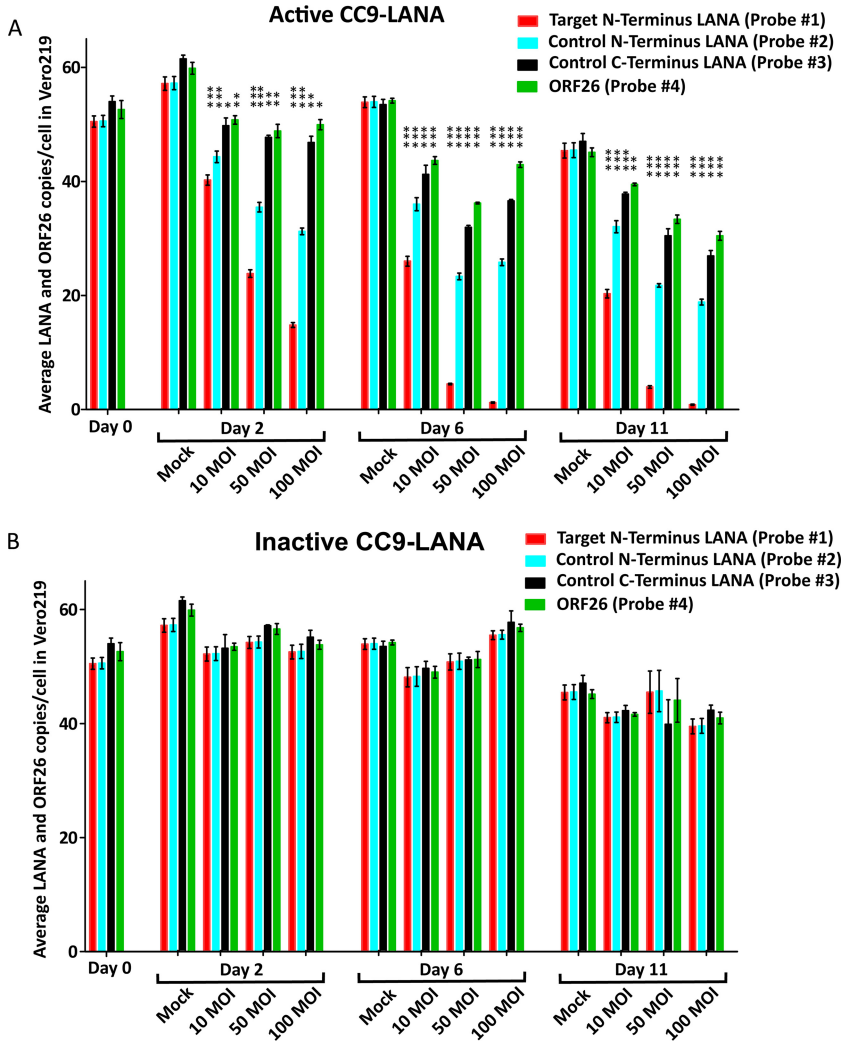

FIG 2 KSHV episome copy number in Vero219 cells transduced with Ad-CC9-LANA or Ad-iCC9-LANA at 10, 50, and 100 MOI over 11 days, as determined by ddPCR. (A) Cells transduced with active CC9-LANA. (B) Cells transduced with inactive CC9-LANA. Statistical significance relative to respective mock is shown by vertical *** (*P* value, <0.0001), vertical ** (*P* value, 0.0003), and vertical * (*P* value, 0.0002). Error bars reflect mean with standard deviation (SD).

linearized. More importantly, the detection of probe number 1 revealed that only 0.7 copies/cell of wild-type LANA remained, demonstrating 97% edited. The LANA and ORF26 copy number in cells transduced with various MOIs of Ad-CC9-LANA were significantly lower than the respective mock cultures at day 11 postransduction (*P* values ranged from =0.0003 to <0.0001).

TABLE 1 Quantification of CC9-LANA effects on KSHV episome

Effect	Formula[a]
Percentage reduction of KSHV episome burden in transduced culture relative to the respective mock (% reduction)	(Mock – P3/P4) ÷ Mock × 100%
Percentage of linearized KSHV episome in transduced culture (% linearized)	(P3/P4 – P2) ÷ P3/P4 × 100%
Percentage of KSHV episome edited by CC9-LANA in transduced culture (% edited)	(P3/P4 – P1) ÷ P3/P4 × 100%

[a]Mock, average episomal copy number per cell in respective mock-transduced culture based on signals from probe numbers 1, 2, 3, and 4; P3/P4, episomal copy number per cell in Ad-CC9-LANA- or Ad-iCC9-LANA-transduced culture based on signals from probe numbers 3 or 4; P2, episomal copy number per cell in Ad-CC9-LANA- or Ad-iCC9-LANA-transduced culture based on signals from probe number 2; P1, episomal copy number per cell in Ad-CC9-LANA- or Ad-iCC9-LANA-transduced culture based on signals from probe number 1.

In comparison, cultures transduced with Ad-iCC9-LANA showed a median 42 KSHV episomal copy number/cell, a quantity that was similar to the mock-transduced culture at the same time point (Fig. 2B). Interestingly, we noted that the copy number derived from probe numbers 2 and 3 was lower than that from the more distal probe number 4 (Fig. 2A). The differences may be due to progressive degradation of the linearized KSHV episome over time. This effect was only observed in cultures transduced with Ad-CC9-LANA.

Effects of CC9-LANA on KSHV episome burden in 32-day transduced cultures. Although the transduction of Ad-CC9-LANA demonstrated a significant reduction in KSHV episome burden in Vero219 within 11 days, it only represented 38% reduction. We reasoned that Cas9-LANA might require more time to achieve a higher reduction level due to the high KSHV copy numbers/cell in Vero219. Therefore, we examined the effects of Cas9-LANA on KSHV episome burden in 32-day transduced cultures of Vero219, together with its parental Vero cells as a control. In parallel, we also studied the effects of Ad-CC9-LANA on a human endothelial cell line, L1T2, which was latently infected with KSHV to serve as the endothelial model (45). The advantages of L1T2 are that unlike primary cells, which cannot recapitulate the long-term latent nature of KSHV infection, and unlike Vero219 cells, L1T2 can maintain latent KSHV infection over an extended period of time without any selective agent, such as puromycin. Moreover, L1T2 has a low viral copy number/cell that resembles the $<$2 viral copies/cell found in KSHV-positive individuals (46). Each cell line (Vero219, Vero, and L1T2) was transduced with 100 MOI of Ad-CC9-LANA or Ad-iCC9-LANA and cultured for 32 days.

To characterize the effects of CC9-LANA on 32-day transduced cells, the KSHV episome burden was followed from day 12 postransduction onward. Similar to the previous 11-day transduction experiment, the Ad-CC9-LANA exerted its function after transduction, and cumulative reductions in KSHV were detected over the study period. At day 12 postransduction in the 32-day transduced cultures of Vero219, while the mock-transduced culture had ~44 LANA and ORF26 copies/cell (Fig. 3A), cells transduced with Ad-CC9-LANA already had significantly lower LANA and ORF26 at ~14 copies/cell, representing a 68% reduction (Fig. 3A). Quantification with probe number 2 at 13 LANA copies/cell, suggested a 7% linearized, whereas quantification of probe number 1 (9 wild-type LANA copies/cell) demonstrated 36% edited at this time point (Fig. 3A). The KSHV episome burden continued to decrease over time. By 32 days postransduction, while the non-puromycin-selected mock-transduced culture had spontaneously decayed to 13 LANA and ORF26 copies/cell, the Ad-CC9-LANA-transduced culture had undergone a 77% reduction with only ~3 LANA and ORF26 copies/cell (Fig. 3A). The LANA and ORF26 copy numbers in Ad-CC9-LAN-transduced cells were all significantly lower than the respective mock cultures (P values, $<$0.0001). In comparison, cultures transduced with Ad-iCC9-LANA showed KSHV episome burden similar to their respective mock-transduced controls (Fig. 3B).

A similar pattern of decreasing KSHV episome burden over time was also observed in L1T2 transduced with Ad-CC9-LANA. At day 12 postransduction, there was only 68% reduction compared with the mock-transduced culture. However, quantification of probe number 1 indicated 86% edited (Fig. 3C). Importantly, an 86% reduction was realized by day 32 postransduction in the Ad-CC9-LANA-transduced culture, with only 0.2 wild-type LANA copies/cell remaining (Fig. 3C). The LANA and ORF26 copy numbers in Ad-CC9-LANA transduced cells were all significantly lower than the respective mock cultures (P values, $<$0.0001). KSHV episome burden was unchanged in Ad-iCC9-LANA and mock-transduced controls (Fig. 3D).

To rule out the possibility that the reduction of KSHV episome burden in Ad-CC9-LANA transduced cultures was due to altered growth kinetics of adenovirus-transduced cells, we monitored the cell viability of the 32-day adenovirus-transduced cultures over time. Our data showed similar growth kinetics of Vero, Vero219, and L1T2, irrespective of transduction status (Fig. 4A to C, respectively). Additionally, since our data showed a significant reduction in KSHV episome burden over time in both Vero219 and L1T2 cells transduced with Ad-CC9-LANA, we investigated whether the observed reductions

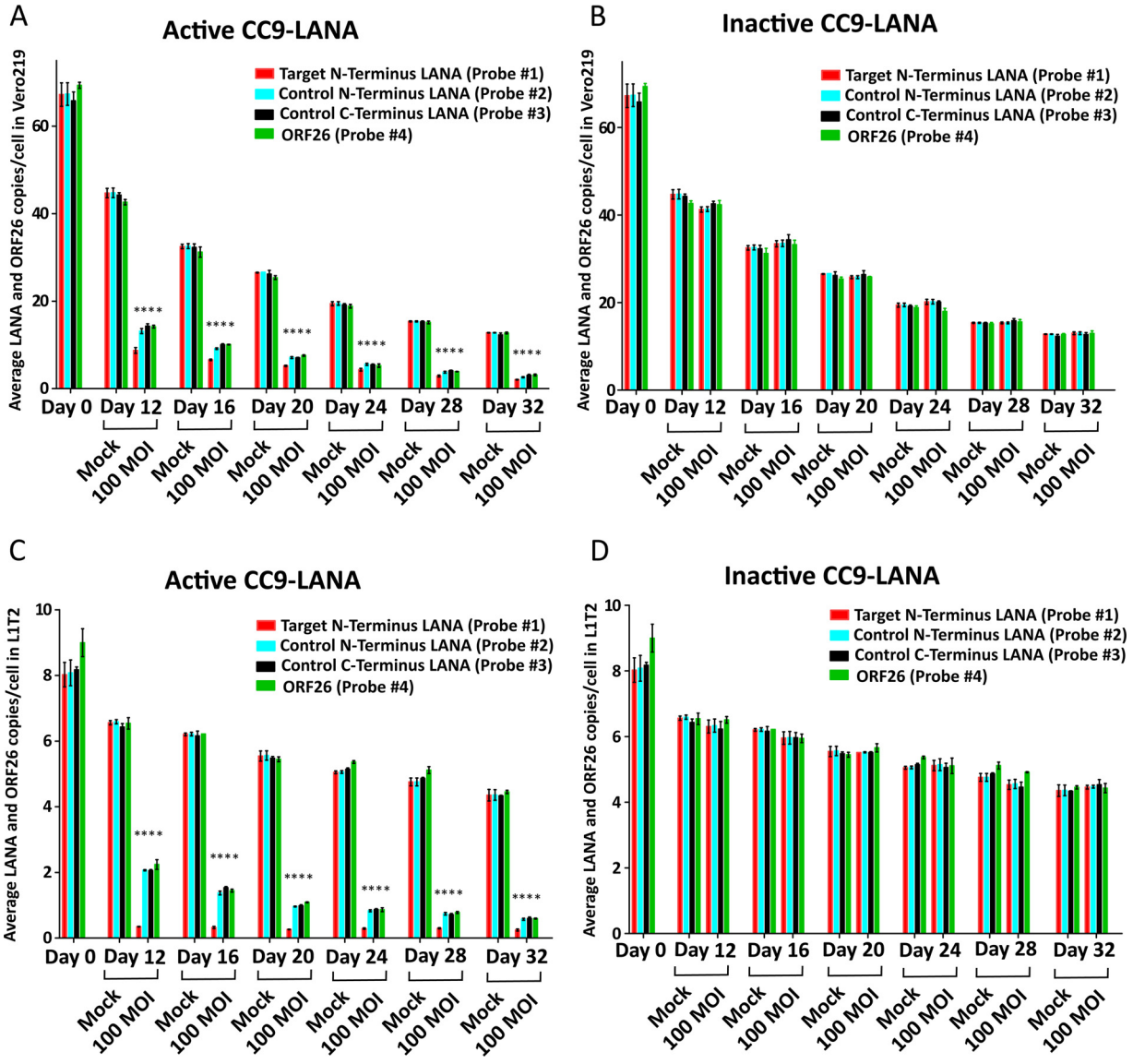

FIG 3 KSHV episome copy number in different cell lines transduced with 100 MOI of Ad-CC9-LANA or Ad-iCC9-LANA over 32 days, as determined by ddPCR. (A) Vero219 transduced with active CC9-LANA. Statistical significance relative to respective mock is shown by vertical * (*P* value, <0.0001). (B) Vero219 transduced with inactive CC9-LANA. (C) L1T2 transduced with active CC9-LANA. Statistical significance relative to respective mock is shown by vertical * (*P* value, <0.0001). (D) L1T2 transduced with inactive CC9-LANA. Error bars reflect mean with SD.

can be reflected at the LANA mRNA expression level. Changes in LANA mRNA expression were measured over time with real-time PCR on cDNA from Ad-CC9-LANA versus Ad-iCC9-LANA or mock-transduced controls. Our data showed a slight increase in LANA mRNA expression relative to mock-transduced culture before a gradual decrease over time in Vero219 and L1T2 cells transduced by Ad-CC9-LANA (Fig. 5A). Importantly, both cell lines showed an ~50% reduction of LANA mRNA expression by 32 days postransduction relative to the mock transduced (Fig. 5A). To ensure that these observations are indeed due to the presence of Cas9 and not spontaneous events, we measured the Cas9 mRNA expression in both cell lines. Both active and inactive CC9-LANA achieved high expression levels, and the Cas9 transcripts was still detectable after 32 days of transduction by Ad-CC9-LANA and Ad-iCC9-LANA (Fig. 5B).

Furthermore, immunohistochemistry (IHC) staining against LANA was performed to confirm that the reduction in KSHV episome burden and LANA mRNA resulted in a temporal loss of KSHV-infected cells from the cultures. Cells from 32 days postrans-

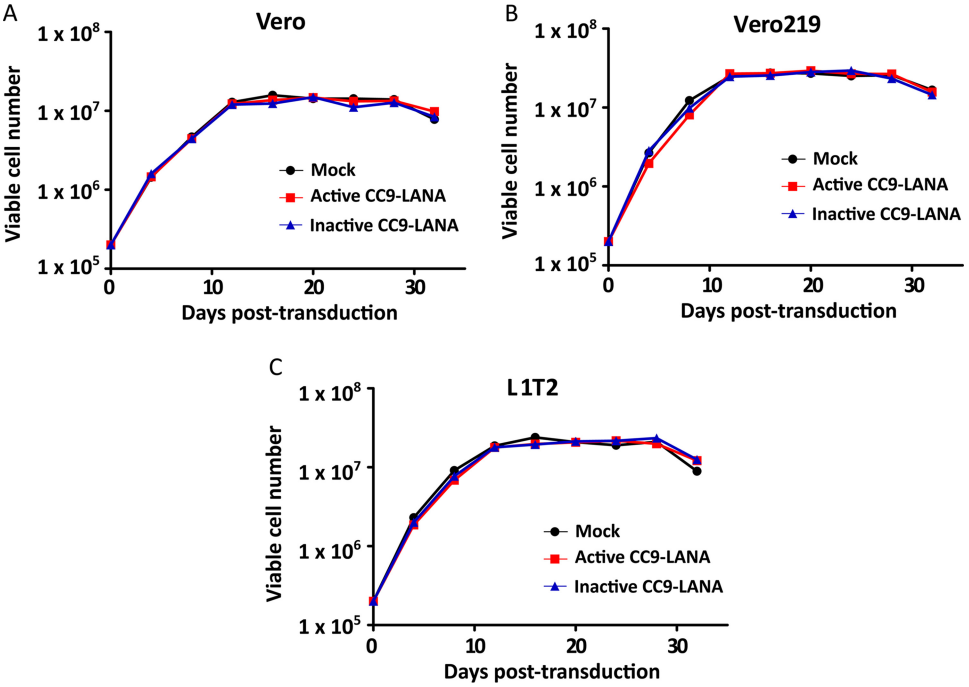

FIG 4 Growth kinetics of different cell lines in 32 days adenovirus transduction with 100 MOI of Ad-CC9-LANA or Ad-iCC9-LANA. (A) Vero. (B) Vero219. (C) L1T2.

duction were allowed to grow in chamber slides for 48 hours before IHC staining for LANA. Since KSHV LANA is a nuclear protein, positive cells can be identified by brown punctate staining within the nuclear boundary. Specificity of the anti-LANA antibody was demonstrated by the lack of LANA staining in uninfected Vero cells (Fig. 6A). Vero219 that were either mock- or Ad-iCC9-LANA-transduced showed strong LANA staining with similar number of KSHV-infected cells at 422 and 430 $LANA^+$ cells/25 fields at $\times$40 magnification, respectively (Fig. 6B). Whereas, Vero219 transduced with Ad-CC9-LANA revealed only 64 $LANA^+$ cells/25 fields (85% reduction) (Fig. 6B). This level of LANA protein reduction was consistent with the levels of episomal loss quantified by ddPCR above. Similar patterns were observed with L1T2 cells that were either mock or Ad-iCC9-LANA transduced, both showed similar numbers of KSHV $LANA^+$ cells/25 fields at 89 and 73, respectively (Fig. 6C). In comparison, L1T2 transduced with Ad-CC9-LANA had $\sim$16 $LANA^+$ cells/25 fields (82% reduction) (Fig. 6C). To further confirm the IHC results, we performed immunoprecipitation for LANA proteins from Vero219 cells at 32 days postransduction. All the major LANA isoforms were observed in the samples; importantly, there are less LANA proteins expressed in the active CC9-LANA than in the mock- and inactive CC9-LANA-transduced cells (Fig. 6D) (47). These results demonstrated that Ad-CC9-LANA can indeed reduce KSHV latency by decreasing the number of KSHV episome in latently infected cells overtime.

Lastly, we sequenced the N terminus of LANA in Ad-CC9-LANA-transduced Vero219 at day 4 postransduction and found a mixture of wild-type and mutated LANA. Importantly, the mutated LANA contained insertion or deletions within the Cas9-targeted site, resulting in a frameshift of the LANA open reading frame and premature stop codon (Fig. 7A and B). This result confirms that Ad-CC9-LANA is indeed functional as it can cleave its intended target site at the N terminus of LANA.

DISCUSSION

The ability of KSHV to establish life-long latent infection has always been a major roadblock for the long-term treatment success of KS, and LANA is the most critical viral protein needed for latency and will be a good target for eliminating KSHV latency. Here, we demonstrated that KSHV latent infections can be reduced by our CC9-LANA system

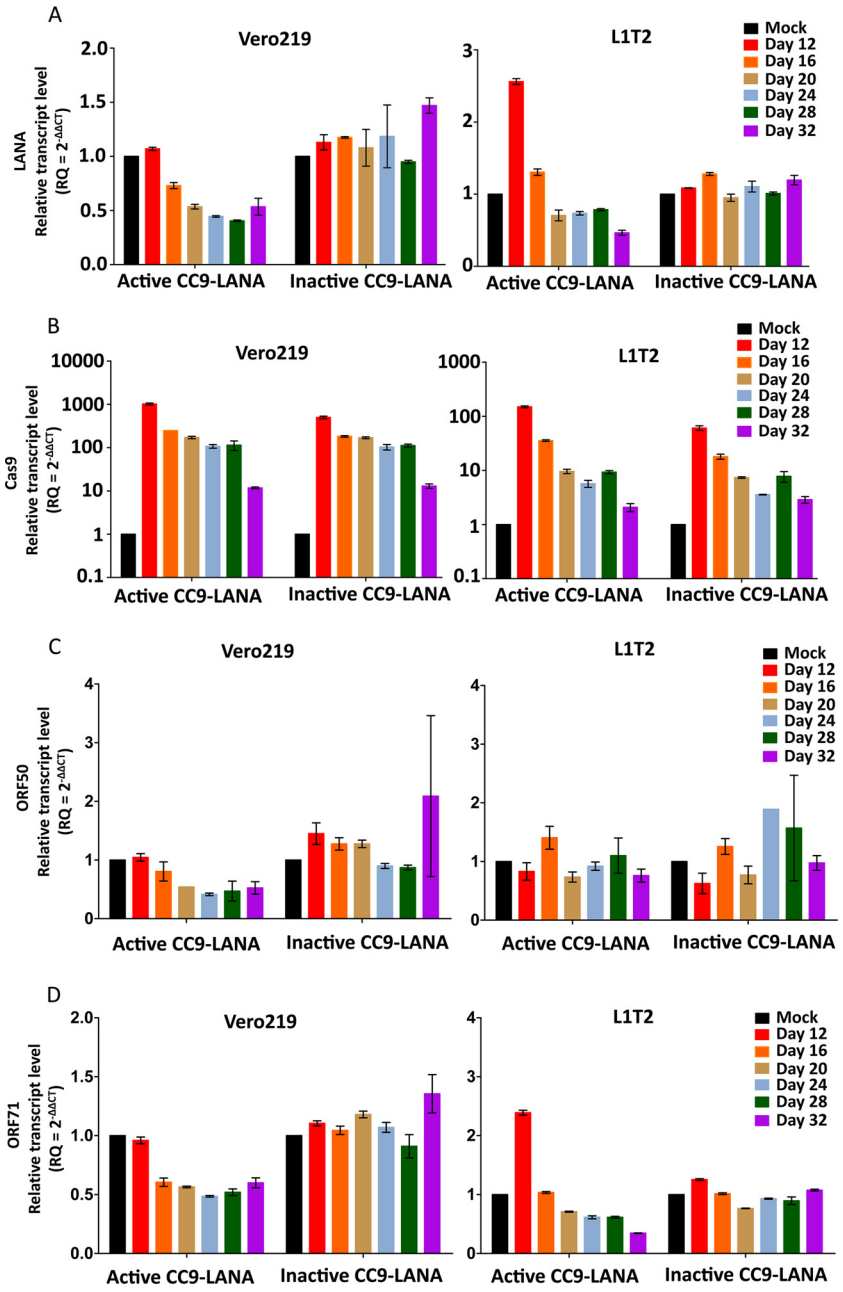

FIG 5 LANA, Cas9, ORF50, and ORF71 transcript levels in Vero219 and L1T2 cells transduced with 100 MOI of Ad-CC9-LANA or Ad-iCC9-LANA over 32 days. (A) LANA. (B) Cas9. (C) ORF50. (D) ORF71. Transcript level was relative to the mock transduced from each respective time point. Error bars reflect mean with SD.

delivered by a replication-incompetent adenovirus type 5. In the Vero219 epithelial cells, a 77% reduction in KSHV episome burden was achieved by day 32 postransduction. A similar action was observed in the L1T2 endothelial cells, which have achieved an impressive 86% reduction in KSHV episome burden by day 32 postransduction. The effectiveness of our Ad-CC9-LANA system is underscored by the fact that KSHV latently infected cells were exposed to adenovirus transduction for only 4 days initially. Yet, the effects of Cas9 were early and enduring, as shown by its mRNA expression at day 32 postransduction.

The fate of the KSHV latently infected cells that lost their KSHV episomes is not known. Our growth kinetic data suggest that losing the KSHV episome will neither affect survival of the once-infected cells nor their replication kinetics. This is likely

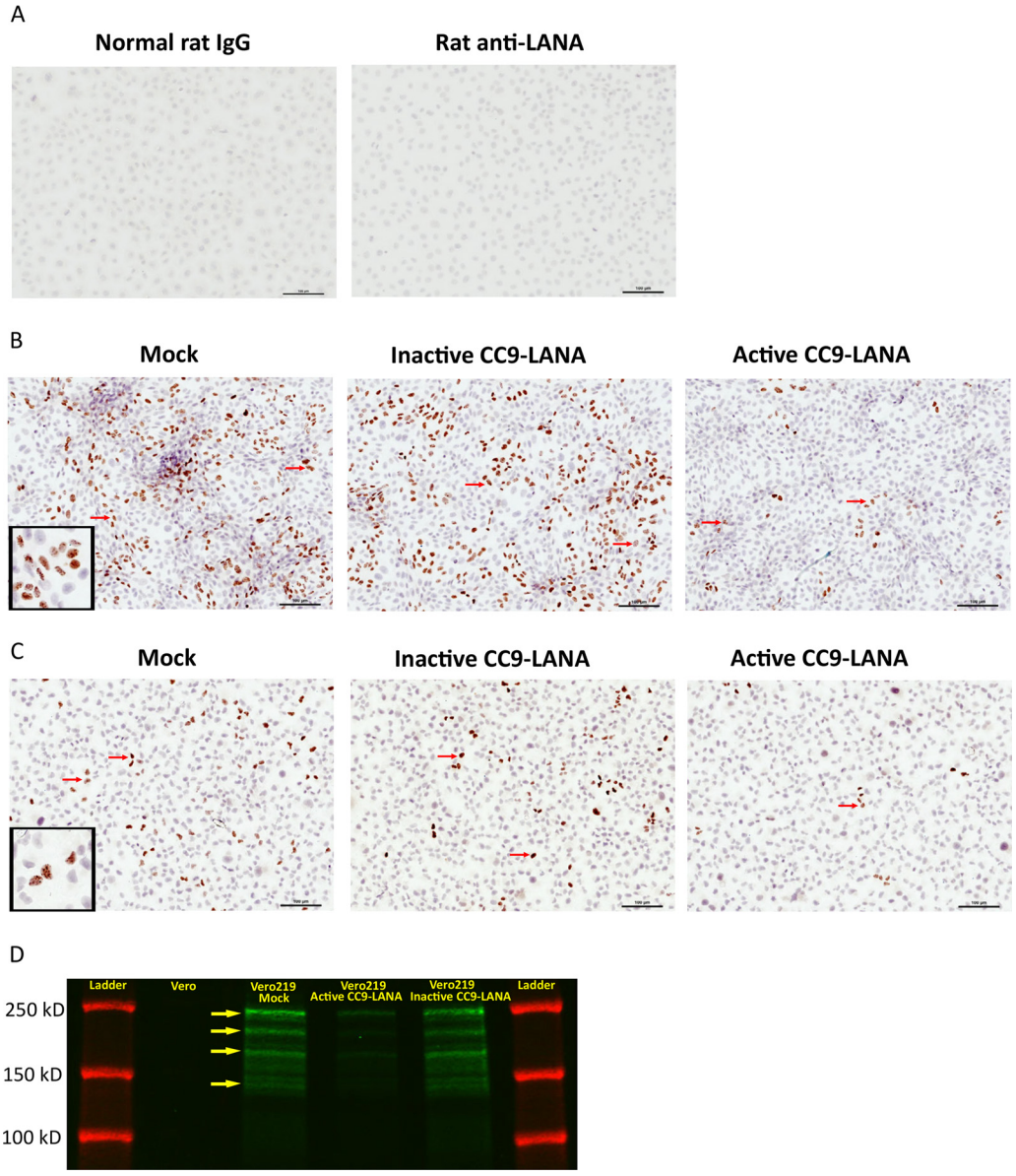

FIG 6 Cells from 32 days postransduction by 100 MOI of Ad-CC9-LANA or Ad-iCC9-LANA were seeded into chamber slides and allowed to grow for 2 days before detection of KSHV LANA by immunohistochemistry. (A) Negative controls of Vero cells stained with normal rat IgG or rat anti-LANA antibody. (B) Vero219 transduced with either mock or inactive or active CC9-LANA. (C) L1T2 transduced with either mock or inactive or active CC9-LANA. Five times 5 fields of pictures (i.e., 25 pictures) were taken at ×40 magnification and digitally stitched for each culture. Red arrows showed examples of LANA$^+$ cells, as indicated by the brown punctate staining within the nuclear boundary. A magnified view was shown at the left lower corner of Vero219 and L1T2 mock transduced to demonstrate the brown punctate staining of LANA within the nucleus. (D) Western blot showing LANA protein expression in mock, active CC9-LANA, and inactive CC9-LANA transduced cells from day 32 samples. KSHV negative Vero cells were used as control. Green color indicates the main LANA isoforms (indicated by yellow arrows). Red color indicates the protein ladder.

because both Vero219 and L1T2 are immortalized cell lines even before infection by KSHV. Hence, their survival will not be KSHV dependent. The same reasoning might also explain the slow spontaneous loss of KSHV episomes in Vero219 in the absence of selective pressure from puromycin. To address this question, primary human endothelial or epithelial cells immortalized by KSHV will be needed. Currently, such cell line does not exist, and our study's ability to address this possibility fully is limited by the availability of such an *in vitro* model. However, our study was able to determine the effects of Ad-CC9-LANA on KSHV episome load. Interestingly, the different episomal copy number derived from probe numbers 3 and 4 suggests that not all episomes

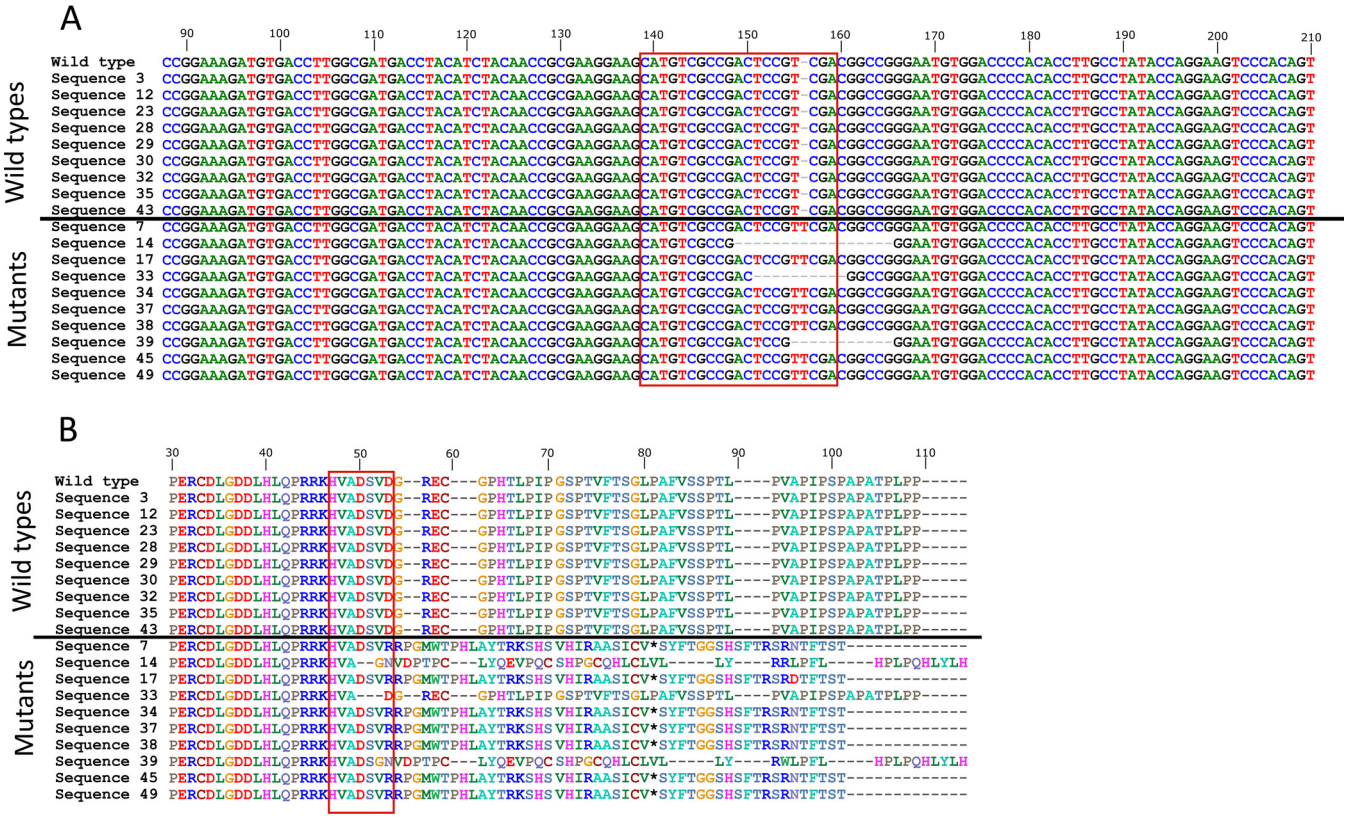

FIG 7 LANA mutations in cells from 4 days postransduction by 100 MOI of Ad-CC9-LANA. (A) Nucleotide sequences alignment of the wild-type LANA with those derived from Ad-CC9-LANA-transduced culture. The Cas9 targeted site at the N terminus of LANA gene is highlighted by the red box. (B) Amino acid sequence alignment of the wild-type LANA with those derived from Ad-CC9-LANA-transduced culture. Sequences above the horizontal lines are wild type and below are mutated sequences. The Cas9 targeted site at the N terminus of LANA gene is highlighted by the red box. *, stop codon.

cleaved by Cas9 were repaired by the host NHEJ pathway. Our data also demonstrated that KSHV episomes with mutated LANA or linearized episomes were present in latently infected cells after CC9-LANA treatment but some were eventually degraded by the host cell. The Ad-CC9-LANA was also tested in BC3 cells, which is a human pleural effusion B lymphoblast infected by KSHV (Fig. 8A and B). Although a similar decrease in viral copy number was observed in BC3 cells, the magnitude is much lower than in Vero219 and L1T2. This is an anticipated result because BC3 cells originated from B cells

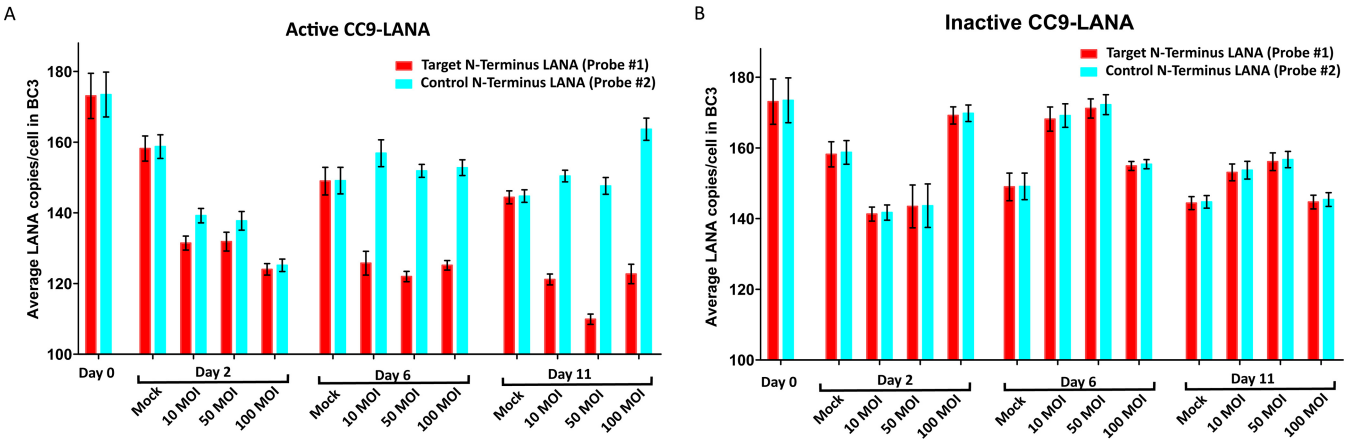

FIG 8 KSHV episome copy number in BC3 cells transduced with Ad-CC9-LANA or Ad-iCC9-LANA at 10, 50, and 100 MOI over 11 days, as determined by ddPCR. (A) Cells transduced with active CC9-LANA. (B) Cells transduced with inactive CC9-LANA.

and do not express the receptor for adenovirus type 5, limiting transduction efficiency. Moreover, BC3 cells contain an extremely high viral copy number of >150 copies per cell. In comparison, the KSHV copy number in actual KS tumor samples ranged from 0.21 to 17.16 copies per cell (48).

Since Cas9 and NHEJ exert their functions on DNA rather than mRNA, the mRNA expression of a targeted gene should not be directly impacted, and any decrease in mRNA would be a result of the decrease in its template DNA level. This pattern was observed in our study with a gradual decrease in both the DNA and mRNA level of KSHV LANA over time, with the exception that LANA mRNA expression slightly increased after adenovirus transduction for about 12 days before gradually decreasing in both Vero219 and L1T2. The actual cause for this observation is not clear, although some studies had suggested that LANA can positively regulate its own expression (49, 50). We hypothesized that when the functional LANA protein level decreased as a result of Cas9, the KSHV episome became untethered from the host chromosomes which increased the accessibility of the LANA promoter to cellular transcriptional machineries and resulted in a higher level of LANA transcripts. Additionally, LANA was reported to repress lytic replication (25). Interestingly, we did not detect any significant increase in lytic gene ORF50 transcripts, but lower transcript expression of another latency-related gene, ORF71, in all transduced cultures (Fig. 5C and D). Importantly, the untethered KSHV episomes would be lost eventually during cell replication, resulting in less KSHV episome burden and LANA mRNA expression. More studies will be necessary to decipher the complex effects that untethering the KSHV episome from host chromosome might have on viral gene expression.

Lastly, the choice of replication-incompetent adenovirus as the delivery vector of our CC9-LANA system was based on its safety over lentiviral vectors. First, adenovirus does not integrate into the host genome, thereby increasing its safety against insertional mutations. Second, adenovirus is a DNA virus which will not have mutations due to reverse transcription. Third, adenovirus will avoid the formation of replication-competent lentiviruses in the presence of wild-type HIV-1, which is a possibility if a lentiviral vector is used in HIV-1-positive patients or animal models. The numerous serotypes of adenoviruses also provide multiple options for overcoming their high seroprevalence among the general population and cell tropism. For instance, a chimpanzee adenovirus had already been used in vaccine design against other human viruses (51).

In conclusion, this is the first study that demonstrated the possibility of reducing KSHV latency with a CC9-LANA system deliverable by an adenovirus type 5 vector. Despite the high rate of reduction in KSHV episome burden achieved by our system in KSHV latently infected cells, we believe its efficiency can be further improved. Work on the second generation of this system with higher efficiency is under way.

MATERIALS AND METHODS

Cell cultures. HEK293 cells were a gift from Eric Weaver. L1T2, Vero, and BC3 cells were obtained from ATCC (number VR-1802, number CCL-81, and number CRL-2277, respectively). HEK293, L1T2, and Vero cells were maintained in Dulbecco's modified Eagle medium (DMEM) with 10% fetal bovine serum (FBS) and 1% penicillin-streptomycin (P/S). BC3 cells were maintained in RPMI with 20% FBS and 1% P/S. Vero219 cells were a gift from Jeffrey Vieira (44) and were maintained in DMEM with 10% FBS, 1% P/S, and 6 μg/ml of puromycin. Puromycin was removed during adenovirus transduction. All cells were maintained at 37°C in a 5% CO_2 incubator.

Construction and preparation of adenovirus vector. The gRNA targeting the N terminus of the LANA gene (5′-CATGTCGCCGACTCCGTCGA-3′) was designed using the optimized CRISPR design tool (41). An oligonucleotide representing the N terminus LANA-specific gRNA was synthesized (Integrated DNA Technologies) and cloned into the phU6-gRNA plasmid (a gift from Charles Gersbach; Addgene number 53188) that expresses the *S. pyogenes* scaffold gRNA from the human U6 promoter (52). The resulted plasmid phU6-NLana encodes an N terminus LANA-specific gRNA under the control of the human U6 promoter. The active form of the human-optimized *S. pyogenes* Cas9 endonuclease was encoded in a separate plasmid, pLV-hUbC-Cas9-T2A-GFP, and an inactive form of the human-optimized *S. pyogenes* Cas9 endonuclease was encoded in a separate plasmid, pLV-hUbC-dCas9-T2A-GFP (gifts from Charles Gersbach; Addgene numbers 53190 and 53191, respectively) (52). To express both the N terminus LANA-specific gRNA and active or inactive form of Cas9 in the same construct, the hU6-NLana and hUbC-Cas9/dCas9-T2A-GFP insert fragments were subcloned into a shuttle vector, pFUW (a gift from

TABLE 2 Primers and probes for ddPCR

Primer or probe	Sequence (5′ to 3′)[a]
Forward primer for probes 1 and 2	AGCCACCGGTAAAGTAGGAC
Reverse primer for probes 1 and 2	GATGTGACCTTGGCGATGAC
Probe 1	FAM-CATGTCGCCGACTCCGTCGA-BHQ1
Probe 2	HEX-TGCTGGCAGCCCGGATG-BHQ1
Forward primer for probe 3	GTGTTGTGGCCTAGCTTTCG
Reverse primer for probe 3	CGCGAATACCGCTATGTACTC
Probe 3	HEX- TCTATCTGTCTGTAAGGGACCGGTGG-BHQ1
Forward primer for probe 4	CGAATCCAACGGATTTGACCTC
Reverse primer for probe 4	CCCATAAATGACACATTGGTGGTA
Probe 4	FAM-CCCATGGTCGTGCCGCAGCA-BHQ1
Forward primer for monkey β-globin probe	CTAGCAACCTCAGACACCATGG
Reverse primer for monkey and human β-globin probes	TCCACGTTCACCTTGCCC
Monkey β-globin probe	HEX-CTCCTGAGGAGAAGACTGCCGTTACCACC-BHQ1
Forward primer for human β-globin probe	CAACCTCAAACAGACACCATGG
Human β-globin probe	HEX-CTCCTGAGGAGAAGTCTGCCGTTACTGCC-BHQ1

[a]FAM, 6-carboxyfluorescein; BHQ1, black hole quencher 1; HEX, hexagonal peroxisome.

David Baltimore; Addgene number 14882) (53). Finally, the N terminus LANA-specific gRNA and active or inactive form of Cas9 were PCR amplified from the shuttle vector using Q5 high-fidelity (HF) DNA polymerase (New England Biolabs) and cloned into the Adeno-X promoterless vector (Clonetech). The adenovirus type 5 vector encoding the N terminus LANA-specific gRNA and active (Ad-CC9-LANA) or inactive (Ad-iCC9-LANA) form of Cas9 were then linearized and transfected into HEK293 cells to generate replication-incompetent adenoviruses, according to the manufacturer's protocol (Clonetech). Adenovirus was harvested by multiple freeze and thaw cycles. The virus titer was determined on HEK293 cells at 72 hours posttransduction by counting GFP-positive cells and calculated using the standard Reed Muench method.

Adenovirus transduction and growth kinetics. For 11-day adenovirus transduction, 1×10^4 Vero219 cells per well were seeded into a 96-well plate with DMEM, 10% FBS, 1% P/S, and 6 μg/ml of puromycin at 24 hours before transduction. A total of 1×10^4 BC3 cells per well were also seeded into a 96-well plate with RPMI, 20% FBS, and 1% P/S at 24 hours before transduction. On the day of transduction, the old medium was removed and either 10, 50, or 100 MOI of Ad-CC9-LANA or Ad-iCC9-LANA was added to the cells without puromycin. The mock culture received only growth medium without puromycin. The 96-well plate was then spun at $400 \times g$ for 20 minutes at room temperature before incubation at 37°C in a 5% CO_2 incubator. For 11-day adenovirus transduction, the cultures were not split and the adenovirus was continuously present until days 2, 6, or 11 postransduction when the cells were washed and harvested for genomic DNA extraction.

For 32-day adenovirus transduction, 2×10^5 Vero, Vero219, or L1T2 cells per well were seeded into a 12-well plate with their respective growth medium at 24 hours before transduction. On the day of transduction, the old medium was removed and 100 MOI of Ad-CC9-LANA or Ad-iCC9-LANA was added. Puromycin was removed from the Vero219 cultures from this time point onward. The mock culture received only growth medium without puromycin. The 12-well plate was then spun at $400 \times g$ for 20 minutes at room temperature before incubation at 37°C in a 5% CO_2 incubator. At day 4 postransduction, the old medium was removed and cells were washed with PBS and fresh medium without adenovirus was added. The 32 days adenovirus-transduced cultures were split, samples were collected, and viability was monitored by Vi-CELL XR cell viability analyzer (Beckman Coulter) every 4 days.

ddPCR. Genomic DNA was extracted from the sample using a Gentra Puregene kit following the manufacturer's protocol (Qiagen). ddPCR was carried out as previously described using the respective primers and probes (Table 2) (54). The collected data were analyzed with QuantaSoft version 1.3.2.0 (Bio-Rad). Cell number was determined with the same procedure, except that primers and probes were changed to target either monkey or human β-globin gene. Each sample was performed in triplicate. Statistical analysis (unpaired *t*-test) was performed using GraphPad Prism 5 (GraphPad Software).

Real-time PCR. Total RNA was extracted from the sample using miRNeasy mini kit (Qiagen) according to the manufacturer's protocol and treated with DNase I. The cDNA was generated with random 9 nonamers and measured with a Qubit ssDNA assay kit (Invitrogen). Real-time PCRs were prepared using iQ SYBR green supermix according to the manufacturer's protocol (Bio-Rad). Each PCR contained 15 ng of cDNA with primer pairs for monkey or human glyceraldehyde-3-phosphate dehydrogenase (GAPDH), LANA, Cas9, ORF50, or ORF71 (Table 3). The PCRs were performed using the QuantStudio3 instrument (Applied Biosystems). All samples were measured in duplicates. The respective GAPDH was used as an internal standard for each target gene. The RNA transcript level for each target gene was presented as relative quantification (RQ) as defined by $2^{-\Delta\Delta CT}$ using the comparative cycle threshold ($\Delta\Delta CT$) method as previously described (55).

Immunohistochemistry and immunoprecipitation of LANA. A total of 5×10^5 cells collected from day 32 postransduction were seeded into 4-well chamber slides in growth medium without puromycin. The slides were washed and fixed in 4% paraformaldehyde at 48 hours postseeding. The fixed slides were washed and incubated in 0.3% H_2O_2 methanol solution for 30 mins at room temperature. The slides were then washed and incubated in sodium citrate solution for 15 mins at 98°C, cooled to room temperature,

TABLE 3 Primers for real-time PCR

Primer	Sequence (5′ to 3′)
Forward primer for monkey and human GAPDH	GAGTCCACTGGCGTCTTCAC
Reverse primer for monkey GAPDH	CCCATGACAAACATAGGGGCGTC
Reverse primer for human GAPDH	ATGACGAACATGGGGGCATC
Forward primer for LANA	TGGATCTCGTCTTCCATCCTTTCCC
Reverse primer for LANA	CCAACAACCACCGGTCCCTT
Forward primer for Cas9	ATGCCGCAGGTGAACATCGT
Reverse primer for Cas9	TGCGATCAGCTTGTCGCTGT
Forward primer for ORF50	GGTGTACAACACATCCACCGCG
Reverse primer for ORF50	TGTCGCAGTAATCACGGCCC
Forward primer for ORF71	GTCTCTGCGACCTGCACGAA
Reverse primer for ORF71	CTCAACCCACACTGGCCCAA

and washed and blocked with 10% normal goat serum for 30 mins at room temperature. After washing, the slides were incubated with rat monoclonal anti-LANA antibody LN35 (Abcam) at 1:25 with blocking solution at 4°C overnight. The next day, the slides were washed and incubated with goat biotinylated anti-rat IgG (Vector Labs) at 1:100 with blocking solution for 1 hour at room temperature. The slides were stained with a Vectorstain ABC kit (Vector Labs) and DAB solution (Dako) according to the manufacturer's protocol. Counterstain was performed using hematoxylin. The stained slides were then air-dried and rinsed twice in xylene solution for 5 mins each. Finally, Cytoseal 60 (Thermo Scientific) and a coverslip were added to the slides. A negative control was performed using normal rat IgG (Vector Labs) and rat monoclonal anti-LANA antibody LN35 with mock-transduced Vero cells. The slides were examined under ×40 magnification with a Nikon Eclipse 50i microscope. Five times 5 fields of pictures (i.e., 25 pictures) were taken with a Nikon DS-Fi3 color camera and stitched and counted using NIS Advanced Elements (Nikon). For immunoprecipitation and Western blot of LANA, Vero219 cells collected from day 32 postransduction were cultured in T-25 flasks until confluent. Cells were collected and lysed with radioimmunoprecipitation assay (RIPA) lysis buffer containing a proteinase inhibitor cocktail. Cellular debris was removed, the amount of total protein was measured by Pierce BCA protein assay (Thermo Scientific), and 400 μg of total protein per sample was used for LANA immunoprecipitation with rat monoclonal anti-LANA (LN35) (Abcam). To detect LANA on Western blot, rat monoclonal anti-LANA (LN35) (Abcam) was used at 1:100 as the primary antibody. For the secondary antibody, goat anti-rat IgG 800CW (Li-Cor Biosciences) was used at 1:10000. The LANA isoforms were visualized with a Odyssey infrared imager (Li-Cor Biosciences).

Sequencing of LANA. The N terminus of LANA was PCR amplified from the genomic DNA of Ad-CC9-LANA-transduced culture at day 4 postransduction with primers (5′-ACTGCGTGGGTGGCAATG-3′ and 5′-TACTGCAGCCTGCTACTGTGTG-3′) and Sanger sequenced by Eurofins Genomics.

ACKNOWLEDGMENTS

This study was supported in part by PHS grants from the National Institutes of Health, National Cancer Institute grants (RO1 CA75903, U54 CA190155, and U54 CA221204), and a National Institute of General Medical Science grant (P30 GM103509) to C.W.

REFERENCES

1. Boshoff C, Weiss RA. 2001. Epidemiology and pathogenesis of Kaposi's sarcoma-associated herpesvirus. Philos Trans R Soc Lond B Biol Sci 356:517–534. https://doi.org/10.1098/rstb.2000.0778.
2. Bayley AC. 1984. Aggressive Kaposi's sarcoma in Zambia, 1983. Lancet 1:1318–1320.
3. Krown SE. 2011. Treatment strategies for Kaposi sarcoma in sub-Saharan Africa: challenges and opportunities. Curr Opin Oncol 23:463–468. https://doi.org/10.1097/CCO.0b013e328349428d.
4. Sengayi MM, Kielkowski D, Egger M, Dreosti L, Bohlius J. 2017. Survival of patients with Kaposi's sarcoma in the South African antiretroviral treatment era: a retrospective cohort study. S Afr Med J 107:871–876. https://doi.org/10.7196/SAMJ.2017.v107i10.12362.
5. Bourboulia D, Aldam D, Lagos D, Allen E, Williams I, Cornforth D, Copas A, Boshoff C. 2004. Short- and long-term effects of highly active antiretroviral therapy on Kaposi sarcoma-associated herpesvirus immune responses and viraemia. AIDS 18:485–493. https://doi.org/10.1097/00002030-200402200-00015.
6. Cesarman E, Chang Y, Moore PS, Said JW, Knowles DM. 1995. Kaposi's sarcoma-associated herpesvirus-like DNA sequences in AIDS-related body-cavity-based lymphomas. N Engl J Med 332:1186–1191. https://doi.org/10.1056/NEJM199505043321802.
7. Soulier J, Grollet L, Oksenhendler E, Cacoub P, Cazals-Hatem D, Babinet P, d'Agay MF, Clauvel JP, Raphael M, Degos L. 1995. Kaposi's sarcoma-associated herpesvirus-like DNA sequences in multicentric Castleman's disease. Blood 86:1276–1280.
8. Dourmishev LA, Dourmishev AL, Palmeri D, Schwartz RA, Lukac DM. 2003. Molecular genetics of Kaposi's sarcoma-associated herpesvirus (human herpesvirus-8) epidemiology and pathogenesis. Microbiol Mol Biol Rev 67:175–212.
9. Reed JA, Nador RG, Spaulding D, Tani Y, Cesarman E, Knowles DM. 1998. Demonstration of Kaposi's sarcoma-associated herpes virus cyclin D homolog in cutaneous Kaposi's sarcoma by colorimetric in situ hybridization using a catalyzed signal amplification system. Blood 91:3825–3832.
10. Staskus KA, Sun R, Miller G, Racz P, Jaslowski A, Metroka C, Brett-Smith H, Haase AT. 1999. Cellular tropism and viral interleukin-6 expression distinguish human herpesvirus 8 involvement in Kaposi's sarcoma, primary effusion lymphoma, and multicentric Castleman's disease. J Virol 73:4181–4187.
11. Regezi JA, MacPhail LA, Daniels TE, DeSouza YG, Greenspan JS, Greenspan D. 1993. Human immunodeficiency virus-associated oral Kaposi's sarcoma. A heterogeneous cell population dominated by spindle-shaped endothelial cells. Am J Pathol 143:240–249.

12. Dedicoat M, Newton R. 2003. Review of the distribution of Kaposi's sarcoma-associated herpesvirus (KSHV) in Africa in relation to the incidence of Kaposi's sarcoma. Br J Cancer 88:1–3. https://doi.org/10.1038/sj.bjc.6600745.
13. Minhas V, Crabtree KL, Chao A, M'Soka TJ, Kankasa C, Bulterys M, Mitchell CD, Wood C. 2008. Early childhood infection by human herpesvirus 8 in Zambia and the role of human immunodeficiency virus type 1 coinfection in a highly endemic area. Am J Epidemiol 168:311–320. https://doi.org/10.1093/aje/kwn125.
14. Ballestas ME, Kaye KM. 2011. The latency-associated nuclear antigen, a multifunctional protein central to Kaposi's sarcoma-associated herpesvirus latency. Future Microbiol 6:1399–1413. https://doi.org/10.2217/fmb.11.137.
15. Baresova P, Pitha PM, Lubyova B. 2013. Distinct roles of Kaposi's sarcoma-associated herpesvirus-encoded viral interferon regulatory factors in inflammatory response and cancer. J Virol 87:9398–9410. https://doi.org/10.1128/JVI.03315-12.
16. Sathish N, Yuan Y. 2011. Evasion and subversion of interferon-mediated antiviral immunity by Kaposi's sarcoma-associated herpesvirus: an overview. J Virol 85:10934–10944. https://doi.org/10.1128/JVI.00687-11.
17. Uppal T, Banerjee S, Sun Z, Verma SC, Robertson ES. 2014. KSHV LANA—the master regulator of KSHV latency. Viruses 6:4961–4998. https://doi.org/10.3390/v6124961.
18. Lukac DM, Yuan Y. 2007. Reactivation and lytic replication of KSHV. *In* Arvin A, Campadelli-Fiume G, Mocarski E, Moore PS, Roizman B, Whitley R, Yamanishi K (ed), Human herpesviruses: biology, therapy, and immunoprophylaxis. Cambridge University Press, Cambridge, United Kingdom.
19. Purushothaman P, Uppal T, Verma SC. 2015. Molecular biology of KSHV lytic reactivation. Viruses 7:116–153. https://doi.org/10.3390/v7010116.
20. Hu J, Garber AC, Renne R. 2002. The latency-associated nuclear antigen of Kaposi's sarcoma-associated herpesvirus supports latent DNA replication in dividing cells. J Virol 76:11677–11687. https://doi.org/10.1128/JVI.76.22.11677-11687.2002.
21. Si H, Verma SC, Lampson MA, Cai Q, Robertson ES. 2008. Kaposi's sarcoma-associated herpesvirus-encoded LANA can interact with the nuclear mitotic apparatus protein to regulate genome maintenance and segregation. J Virol 82:6734–6746. https://doi.org/10.1128/JVI.00342-08.
22. Ford PW, Bryan BA, Dyson OF, Weidner DA, Chintalgattu V, Akula SM. 2006. Raf/MEK/ERK signalling triggers reactivation of Kaposi's sarcoma-associated herpesvirus latency. J Gen Virol 87:1139–1144. https://doi.org/10.1099/vir.0.81628-0.
23. Friborg J, Jr, Kong W, Hottiger MO, Nabel GJ. 1999. p53 inhibition by the LANA protein of KSHV protects against cell death. Nature 402:889–894. https://doi.org/10.1038/47266.
24. Lan K, Kuppers DA, Robertson ES. 2005. Kaposi's sarcoma-associated herpesvirus reactivation is regulated by interaction of latency-associated nuclear antigen with recombination signal sequence-binding protein Jkappa, the major downstream effector of the Notch signaling pathway. J Virol 79:3468–3478. https://doi.org/10.1128/JVI.79.6.3468-3478.2005.
25. Lan K, Kuppers DA, Verma SC, Robertson ES. 2004. Kaposi's sarcoma-associated herpesvirus-encoded latency-associated nuclear antigen inhibits lytic replication by targeting Rta: a potential mechanism for virus-mediated control of latency. J Virol 78:6585–6594. https://doi.org/10.1128/JVI.78.12.6585-6594.2004.
26. Muromoto R, Okabe K, Fujimuro M, Sugiyama K, Yokosawa H, Seya T, Matsuda T. 2006. Physical and functional interactions between STAT3 and Kaposi's sarcoma-associated herpesvirus-encoded LANA. FEBS Lett 580:93–98. https://doi.org/10.1016/j.febslet.2005.11.057.
27. Radkov SA, Kellam P, Boshoff C. 2000. The latent nuclear antigen of Kaposi sarcoma-associated herpesvirus targets the retinoblastoma-E2F pathway and with the oncogene Hras transforms primary rat cells. Nat Med 6:1121–1127. https://doi.org/10.1038/80459.
28. Doudna JA, Charpentier E. 2014. Genome editing. The new frontier of genome engineering with CRISPR-Cas9. Science 346:1258096. https://doi.org/10.1126/science.1258096.
29. Kennedy EM, Kornepati AV, Goldstein M, Bogerd HP, Poling BC, Whisnant AW, Kastan MB, Cullen BR. 2014. Inactivation of the human papillomavirus E6 or E7 gene in cervical carcinoma cells by using a bacterial CRISPR/Cas RNA-guided endonuclease. J Virol 88:11965–11972. https://doi.org/10.1128/JVI.01879-14.
30. Li Z, Bi Y, Xiao H, Sun L, Ren Y, Li Y, Chen C, Cun W. 2018. CRISPR-Cas9 system-driven site-specific selection pressure on herpes simplex virus genomes. Virus Res 244:286–295. https://doi.org/10.1016/j.virusres.2017.03.010.
31. van Diemen FR, Kruse EM, Hooykaas MJ, Bruggeling CE, Schurch AC, van Ham PM, Imhof SM, Nijhuis M, Wiertz EJ, Lebbink RJ. 2016. CRISPR/Cas9-mediated genome editing of herpesviruses limits productive and latent infections. PLoS Pathog 12:e1005701. https://doi.org/10.1371/journal.ppat.1005701.
32. Yuen KS, Chan CP, Wong NH, Ho CH, Ho TH, Lei T, Deng W, Tsao SW, Chen H, Kok KH, Jin DY. 2015. CRISPR/Cas9-mediated genome editing of Epstein-Barr virus in human cells. J Gen Virol 96:626–636. https://doi.org/10.1099/jgv.0.000012.
33. Yuen KS, Wang ZM, Wong NM, Zhang ZQ, Cheng TF, Lui WY, Chan CP, Jin DY. 2018. Suppression of Epstein-Barr virus DNA load in latently infected nasopharyngeal carcinoma cells by CRISPR/Cas9. Virus Res 244:296–303. https://doi.org/10.1016/j.virusres.2017.04.019.
34. Kaminski R, Chen Y, Fischer T, Tedaldi E, Napoli A, Zhang Y, Karn J, Hu W, Khalili K. 2016. Elimination of HIV-1 genomes from human T-lymphoid cells by CRISPR/Cas9 gene editing. Sci Rep 6:22555. https://doi.org/10.1038/srep22555.
35. Kelley-Clarke B, Ballestas ME, Komatsu T, Kaye KM. 2007. Kaposi's sarcoma herpesvirus C-terminal LANA concentrates at pericentromeric and peri-telomeric regions of a subset of mitotic chromosomes. Virology 357:149–157. https://doi.org/10.1016/j.virol.2006.07.052.
36. Vázquez EDL, Carey VJ, Kaye KM. 2013. Identification of Kaposi's sarcoma-associated herpesvirus LANA regions important for episome segregation, replication, and persistence. J Virol 87:12270–12283. https://doi.org/10.1128/JVI.01243-13.
37. Godfrey A, Anderson J, Papanastasiou A, Takeuchi Y, Boshoff C. 2005. Inhibiting primary effusion lymphoma by lentiviral vectors encoding short hairpin RNA. Blood 105:2510–2518. https://doi.org/10.1182/blood-2004-08-3052.
38. Nelson CE, Hakim CH, Ousterout DG, Thakore PI, Moreb EA, Rivera RMC, Madhavan S, Pan X, Ran FA, Yan WX, Asokan A, Zhang F, Duan D, Gersbach CA. 2016. In vivo genome editing improves muscle function in a mouse model of Duchenne muscular dystrophy. Science 351:403–407. https://doi.org/10.1126/science.aad5143.
39. Yang Y, Wang L, Bell P, McMenamin D, He Z, White J, Yu H, Xu C, Morizono H, Musunuru K, Batshaw ML, Wilson JM. 2016. A dual AAV system enables the Cas9-mediated correction of a metabolic liver disease in newborn mice. Nat Biotechnol 34:334–338. https://doi.org/10.1038/nbt.3469.
40. Yin H, Song CQ, Dorkin JR, Zhu LJ, Li Y, Wu Q, Park A, Yang J, Suresh S, Bizhanova A, Gupta A, Bolukbasi MF, Walsh S, Bogorad RL, Gao G, Weng Z, Dong Y, Koteliansky V, Wolfe SA, Langer R, Xue W, Anderson DG. 2016. Therapeutic genome editing by combined viral and non-viral delivery of CRISPR system components in vivo. Nat Biotechnol 34:328–333. https://doi.org/10.1038/nbt.3471.
41. Hsu PD, Scott DA, Weinstein JA, Ran FA, Konermann S, Agarwala V, Li Y, Fine EJ, Wu X, Shalem O, Cradick TJ, Marraffini LA, Bao G, Zhang F. 2013. DNA targeting specificity of RNA-guided Cas9 nucleases. Nat Biotechnol 31:827–832. https://doi.org/10.1038/nbt.2647.
42. Qin JY, Zhang L, Clift KL, Hulur I, Xiang AP, Ren BZ, Lahn BT. 2010. Systematic comparison of constitutive promoters and the doxycycline-inducible promoter. PLoS One 5:e10611. https://doi.org/10.1371/journal.pone.0010611.
43. Zhang XH, Tee LY, Wang XG, Huang QS, Yang SH. 2015. Off-target effects in CRISPR/Cas9-mediated genome engineering. Mol Ther Nucleic Acids 4:e264. https://doi.org/10.1038/mtna.2015.37.
44. Vieira J, O'Hearn PM. 2004. Use of the red fluorescent protein as a marker of Kaposi's sarcoma-associated herpesvirus lytic gene expression. Virology 325:225–240. https://doi.org/10.1016/j.virol.2004.03.049.
45. Roy D, Sin SH, Lucas A, Venkataramanan R, Wang L, Eason A, Chavakula V, Hilton IB, Tamburro KM, Damania B, Dittmer DP. 2013. mTOR inhibitors block Kaposi sarcoma growth by inhibiting essential autocrine growth factors and tumor angiogenesis. Cancer Res 73:2235–2246. https://doi.org/10.1158/0008-5472.CAN-12-1851.
46. Lallemand F, Desire N, Rozenbaum W, Nicolas JC, Marechal V. 2000. Quantitative analysis of human herpesvirus 8 viral load using a real-time PCR assay. J Clin Microbiol 38:1404–1408.
47. Garrigues HJ, Howard K, Barcy S, Ikoma M, Moses AV, Deutsch GH, Wu D, Ueda K, Rose TM. 2017. Full-length isoforms of Kaposi's sarcoma-associated herpesvirus latency-associated nuclear antigen accumulate in

the cytoplasm of cells undergoing the lytic cycle of replication. J Virol 91:e01532-17. https://doi.org/10.1128/JVI.01532-17.
48. Olp LN, Jeanniard A, Marimo C, West JT, Wood C. 2015. Whole-genome sequencing of Kaposi's sarcoma-associated herpesvirus from Zambian Kaposi's sarcoma biopsy specimens reveals unique viral diversity. J Virol 89:12299–12308. https://doi.org/10.1128/JVI.01712-15.
49. Jeong J, Papin J, Dittmer D. 2001. Differential regulation of the overlapping Kaposi's sarcoma-associated herpesvirus vGCR (orf74) and LANA (orf73) promoters. J Virol 75:1798–1807. https://doi.org/10.1128/JVI.75.4.1798-1807.2001.
50. Jeong JH, Orvis J, Kim JW, McMurtrey CP, Renne R, Dittmer DP. 2004. Regulation and autoregulation of the promoter for the latency-associated nuclear antigen of Kaposi's sarcoma-associated herpesvirus. J Biol Chem 279:16822–16831. https://doi.org/10.1074/jbc.M312801200.
51. Ledgerwood JE, DeZure AD, Stanley DA, Coates EE, Novik L, Enama ME, Berkowitz NM, Hu Z, Joshi G, Ploquin A, Sitar S, Gordon IJ, Plummer SA, Holman LA, Hendel CS, Yamshchikov G, Roman F, Nicosia A, Colloca S, Cortese R, Bailer RT, Schwartz RM, Roederer M, Mascola JR, Koup RA, Sullivan NJ, Graham BS, Team VRCS. 2017. Chimpanzee adenovirus vector Ebola vaccine. N Engl J Med 376:928–938. https://doi.org/10.1056/NEJMoa1410863.
52. Kabadi AM, Ousterout DG, Hilton IB, Gersbach CA. 2014. Multiplex CRISPR/Cas9-based genome engineering from a single lentiviral vector. Nucleic Acids Res 42:e147. https://doi.org/10.1093/nar/gku749.
53. Lois C, Hong EJ, Pease S, Brown EJ, Baltimore D. 2002. Germline transmission and tissue-specific expression of transgenes delivered by lentiviral vectors. Science 295:868–872. https://doi.org/10.1126/science.1067081.
54. Tso FY, Kang G, Kwon EH, Julius P, Li Q, West JT, Wood C. 2018. Brain is a potential sanctuary for subtype C HIV-1 irrespective of ART treatment outcome. PLoS One 13:e0201325. https://doi.org/10.1371/journal.pone.0201325.
55. Tso FY, Kossenkov AV, Lidenge SJ, Ngalamika O, Ngowi JR, Mwaiselage J, Wickramasinghe J, Kwon EH, West JT, Lieberman PM, Wood C. 2018. RNA-Seq of Kaposi's sarcoma reveals alterations in glucose and lipid metabolism. PLoS Pathog 14:e1006844. https://doi.org/10.1371/journal.ppat.1006844.